A practical method for estimating the light backscattering coefficient from the remote-sensing reflectance in Baltic Sea conditions and examples of its possible application

Sławomir B. Woźniak*, Mirosław Darecki, Sławomir Sagan

Institute of Oceanology, Polish Academy of Sciences, ul. Powstańców Warszawy 55, 81-712 Sopot, Poland

**corresponding author*: woznjr@iopan.gda.pl

INTRODUCTION

The paper discusses a simple empirical method for calculating spectra of the light backscattering coefficient $b_b(\lambda)$ in Baltic Sea surface waters based on the remote-sensing reflectance $R_{rs}(\lambda)$. This method relies on the following two aspects: 1) the existence of a relatively strong statistical correlation between these two optical quantities in the red light wavelength range (e.g. at 620 nm), and 2) the fact that backscattering coefficients at other wavelengths can be approximated from their values estimated in the red part of the spectrum. Possible applications are described. This method is applicable as one of the stages in simple algorithms for estimating spectra of the light absorption coefficient in seawater, without the need for any *a priori* assumptions regarding the spectral shape of absorption by dissolved and suspended seawater constituents.

MATERIAL AND METHODS

Our simple method was developed on the basis of empirical data gathered in surface waters of the southern and central Baltic Sea, at 148 stations during 6 short cruises of r/v "Oceania" in spring (April 2011, May 2013, 2014, 2015) and late summer (September 2011, 2012) (for the positions of the measurement stations, see Figure 1a). *In situ* optical measurements included spectral values of the light backscattering coefficient in seawater b_b, the light absorption coefficient by all non-water constituents of seawater a_n, and the remote-sensing reflectance R_{rs}.

The backscattering coefficient $b_b(\lambda)$ [m^{-1}] was measured *in situ* in surface water layer with HydroScat-4 instrument (HOBI Labs) at 4 wavelengths: 420, 488, 550, 620 nm (methods described by Maffione and Dana (1997) and Dana and Maffione (2002) were used. A standard method of correction for incomplete recovery of the light backscattered in highly attenuating waters was also applied (the so-called sigma correction, see User's Manual (HOBI Labs, 2008)). To obtain values of backscattering of light by suspended particles only, $b_{bp}(\lambda)$, theoretical values of backscattering coefficient for pure water $b_w(\lambda)$ were subtracted according to Morel (1974).

The light absorption coefficient by all non-water (suspended and dissolved) constituents of seawater $a_n(\lambda)$ [m^{-1}] was measured *in situ* in surface water layer with use of

AC-9 instrument (WET Labs) at 9 wavelengths: 412, 440, 488, 510, 532, 555, 650, 676, and 715 nm. The standard methods of corrections were applied for temperature and salinity effects (Pegau et al. (1997)), and for the incomplete recovery of the scattered light in the absorption tube (the so-called proportional method, Zaneveld et al. (1994)). The $a_n(715)$ assumed to be 0. To obtain values of $a(\lambda)$ (total light absorption coefficient of seawater) values of absorption coefficient for pure water $a_w(\lambda)$ were added (taken from Pope and Fry (1997), Sogandares and Fry (1997) and Smith and Backer (1981)).

The remote-sensing reflectance just above seawater $R_{rs}(\lambda)$ [sr^{-1}] was calculated from results of radiometric measurements performed *in situ* with use of C-OPS instrument (Biospherical Instruments Inc.) at 17 wavelengths from 340 to 765 nm. Directly measured were the downward irradiance just above the water $E_d\,(0^+,\lambda)$, and the upward irradiance profiles in water $L_u(z,\lambda)$ (the correction for the self-shading effect was applied according to Gordon and Ding (1992) and Zibordi and Ferrari (1995)). The estimated quantity was the water leaving radiance $L_w(0^+,\lambda)$. The reflectance $R_{rs}(\lambda)$ was calculated as $L_w(0^+,\lambda)$ / $E_d\,(0^+,\lambda)$.

The original *in situ* measurements, when necessary, were appropriately interpolated (or extrapolated) to eleven spectral bands: 412, 440, 488, 510, 532, 555, 589, 620, 650, 676, 715, to enable further quantitative analysis.

In general, the variability of all optical quantities in the data set subsequently analysed was around one order of magnitude or more. Changes in the spectral shapes of the remote-sensing reflectance $R_{rs}(\lambda)$ and the light absorption coefficient $a(\lambda)$ were also significant (see Figure 1b).

RESULTS AND DISCUSSION

Apart from the complex relationships that can theoretically occur between given apparent optical properties (on the basis of which the remote-sensing reflectance R_{rs} is defined) and inherent optical properties describing light scattering and absorption by various components of seawater, here we decided to statistically analyse the dependences between measured values of b_b and reflectance R_{rs}. It turned out that, in contrast to the blue light bands, approximate relationships between the logarithms of these two quantities can be derived for longer wavelengths, especially in the red, in the form of a second-order polynomial. From the statistical point of view the best relationship was found for the 620 nm band (see Figure 2a):

$$\log(b_b(620)) = 0.4369\,(\log(R_{rs}(620)))^2 + 3.7597\,(\log(R_{rs}(620))) + 5.0813,\ (r^2 = 0.90) \qquad (1)$$

In addition, we analysed the changes in the spectral shape of the backscattering coefficient of particles b_{bp} (see Figure 2b). Generally, we found these changes to be relatively small when compared with the changes in the magnitude of b_{bp} between different samples. Rather than directly using the $b_b(\lambda)$ *vs* $R_{rs}(\lambda)$ relationships in order to get a rough estimate of b_b at wavelengths other than 620 nm, it is better first to estimate $b_b(620)$ with equation (1), and then use it in the next step to calculate $b_b(\lambda)$ by assuming the typical unchanging spectral shape of the b_{bp} spectrum (like the one denoted as average shape in Figure 2b). However, in order to improve the accuracy slightly, the changing slopes of the b_{bp} spectrum should also be taken into account. When we matched the classic power functions to all of our b_{bp} spectra (functions of the following form: $b_{bp}(\lambda) = b_{bp}(\lambda_{ref})\ (\lambda_{ref}/\lambda)^{\gamma}$, matched to pass exactly through $b_{bp}(420)$ and $b_{bp}(620)$ values), we found the typical slope γ (a median value) to be 1.08. The 10th and 90th percentiles of γ were 0.51 and 1.8 respectively. But we noticed that in most cases such a standard fit was not an exact spectral representation of our data. Most of our spectra exhibited features similar to those on the average spectrum, i.e. a small concavity in the blue and a convexity in the green light wavelengths (note that the original b_b values were measured at only four wavelengths). For that reason, we decided to apply a "hybrid" description that combined both of the above observations, i.e. the variation of the spectral slopes of b_{bp}, and the generally observed deviations from the "smooth" power function shapes. Finally, considering the contribution from pure water, the sought-after coefficient $b_b(\lambda)$ could be approximated using the following equation:

$$b_b(\lambda) = (b_b(620) - b_{bw}(620))\ C_1(\lambda)\ (620/\lambda)^{\gamma} + b_{bw}(\lambda) \qquad (2)$$

In this equation, C_1 is an empirical factor adjusting the power function to the average shape of b_{bp} observed in our measurements. Its numerical values obtained for our data set are as follows:

λ	412	440	488	510	532	555	589	620	650	676	715
$C_1(\lambda)$	1.01	1.02	1.02	1.06	1.09	1.11	1.06	1	0.93	0.86	0.74

As regards the slope parameter γ in equation (2), we found that, having tested different approaches (e.g. correlations with estimated $b_{bp}(620)$ values or with different reflectance ratios), it may be correlated rather roughly with the spectral ratio of the remote-sensing reflectance just below the sea surface r_{rs} for the bands at 510 and 555 nm (see Figure 2c):

$$\gamma = 1.6379\ (r_{rs}(510)/r_{rs}(555)) - 0.3104, \quad (r^2 = 0.25) \qquad (3)$$

For this particular purpose, the r_{rs} values were calculated from the "above water" reflectance $R_{rs}(\lambda)$ according to the simplified formula given by Lee et al. (2002): $r_{rs}(\lambda) = R_{rs}(\lambda)/(0.52 + 1.7\ R_{rs}(\lambda)))$. Our calculations also took into account backscattering by pure water according to the formula given by Morel (1974): $b_{bw}(\lambda)\ [m^{-1}] = 0.000899\ (\lambda/525)^{-4.34}$.

The values of $b_b(\lambda)$ retrieved using the proposed simple calculation method (combined equations (1) – (3)) were compared with the original set of measured/interpolated values (see Figure 3a). The accuracy of retrieval/estimation can be characterized by the practically negligible systematic errors and the moderate statistical errors. The standard error factor, i.e. the statistical quantity characterizing the statistical error according to logarithmic statistics, calculated for our retrieved values of $b_b(\lambda)$, varies from 1.23 to 1.28, depending on the light wavelength. This means that the relative statistical error ranges at worst from -22% to +28%. Such an accuracy, although far from perfect, seems reasonable when we see that the variability of backscattering coefficients measured in the target waters covered more than one order of magnitude.

If backscattering spectra can be estimated with reasonable accuracy, we might also wish to retrieve other information contained in the remote-sensing reflectance spectra. Table 1 presents two examples of simple algorithms that combine the simple method for calculating b_b (or its slightly modified version) with some other empirical and analytical steps, finally leading to the estimated spectra of the light absorption coefficient in seawater. The first example is a less complicated algorithm – A, which contains only four steps. The first two steps, A1 and A2, estimate b_b at the red-light wavelength, then at other wavelengths (exactly according to formulas (1) – (3)). Step A3 is also empirical: here we propose to estimate the ratio of the backscattering coefficient to the sum of absorption and backscattering coefficients (i.e. $u(\lambda) = b_b(\lambda)/(a(\lambda) + b_b(\lambda))$) directly from R_{rs} spectra. We discuss three variants of this step. In the first two we assume that the relationship between R_{rs} and u should be universal, regardless of the light wavelength (see the empirical equations plotted in Figure 4a). The third variant is different: here, fixed average values of the ratio of the target quantities are assigned to individual spectral bands (see Figure 4b). In practice, the latter variant proved to yield the most accurate results. Algorithm A contains a final analytical step A4, in which the light absorption coefficients $a(\lambda)$ and $a_n(\lambda)$ can be calculated from values of $b_b(\lambda)$ and $u(\lambda)$ estimated earlier. Table 1 also presents the slightly more complex five-step algorithm B, in which the order of calculations seems better justified from the point of view of the physics of the phenomena described. Step B1 of this algorithm calculates the remote-sensing reflectance "just below" the surface, $r_{rs}(\lambda)$, from values of $R_{rs}(\lambda)$ defined as "just above" the surface (according to the aforementioned formula by Lee et al. (2002)). Step B2 estimates $u(\lambda)$ from $r_{rs}(\lambda)$. This step is presented in three different variants. The first two use estimated relationships matched to all our data regardless of the light wavelength (see Figure 4c). In the third one, again the most accurate one, we assigned average values of the ratio of the target quantities for the individual spectral bands. The next step, B3, estimates b_b at the red light wavelength, but this time as a function of $u(620)$ (see Figure 4d and the equation presented there; note that all three steps, from B1 to B3, together represent an alternative way of estimating $b_b(620)$, compared to the simplified relationship given by equation (1)). The last two steps, B4 and B5, are the same as steps A2 and A4 of algorithm A. In these last two steps the spectral values of b_b are estimated, after which $a(\lambda)$ and $a_n(\lambda)$ are calculated analytically.

The precision achievable with the simple algorithm A, is characterized by statistical parameters given in Table 2a. Since algorithm A uses directly equations from (1) to (3), the accuracy of b_b retrieval is exactly as we mentioned earlier: the practically negligible systematic error and the moderate statistical errors, characterized by the standard error factor, from 1.23 to 1.28 depending on the light wavelength. With regard to total absorption coefficients $a(\lambda)$ the systematic errors of its estimation are also quite low (lower than +5% at most of the examined light wavelengths), and the values of the standard error factors are moderate (between 1.09 and 1.28). The situation is somewhat different in the case of the absorption coefficient of all non-water constituents $a_n(\lambda)$. Apparently in line with general expectations, the accuracy of estimating a_n estimation is poorer in the spectral regions where absorption by pure water dominates the total absorption (see Figure 3b). But when the contribution from pure water is relatively small, the systematic errors of a_n are low and the standard error factors are still reasonable (between 1.25 and 1.34) for light wavelengths equal to or shorter than 555 nm. The precision of the slightly more complex algorithm B is generally similar. The accuracy of estimates of $b_b(\lambda)$ is only slightly worse than with algorithm A, and is similar or slightly better when $a(\lambda)$ and $a_n(\lambda)$ are retrieved (see Table 2b). For an additional assessment of our algorithms, we made an initial comparison with one of the algorithms commonly used by the ocean-colour community. We performed a similar accuracy assessment when estimating the inherent optical properties of seawater using one of the latest versions of the Quasi-Analytical Algorithm (QAA) (see e.g. Lee et al. (2002), IOCCG (2006); for the description of QAA_v6, see: *http://ioccg.org/resources/software/*). It turns out that the retrieval accuracy of b_b and a_n with the latter algorithm may be much worse at some wavelengths when compared to our simple alternatives (see Table 2c).

SUMMARY

The simple method of calculating the backscattering coefficient presented in this short paper is strictly empirical. We believe that, at least for the Baltic Sea or similar conditions, it may be a practical alternative to other, often more complex methods of retrieving inherent optical properties. Obviously, this method should only be used in situations when reliable information on the remote-sensing-reflectance in the red light range of wavelengths is available. The two examples of algorithms that use our empirical method as one of their stages can be treated as alternatives to other existing semi-analytical inversion approaches used in the analysis of ocean-colour data. The two examples shown can generally be assigned to the "spectral deconvolution" class (for a current overview of approaches for retrieving marine inherent optical properties, see e.g. Werdell et al. (2018)). This particular class of semi-analytical algorithms enables one to determine the total absorption coefficients first, without *a priori* assumptions about spectral shapes of absorption by certain seawater constituents. For that reason, spectral deconvolution methods can be used to explore multiple approaches for further decomposing light absorption spectra. We believe that in the case of the Baltic Sea, where significant seasonal changes in phytoplankton absorption properties take place (see e.g. the extended abstract by Meler et al. (2018) in the same volume), different spectral deconvolution methods should be further developed.

REFERENCES

Dana, D.R, and R.A. Maffione, 2002. Determining the Backward Scattering Coefficient with Fixed-Angle Backscattering Sensors – Revisited. Presentation from Ocean Optics XVI conference, Santa Fe, New Mexico, November 18-22, 2002.

Gordon, H.R., and K. Ding, 1992. Self-shading of in-water instruments. Limnology and Oceanography 37(3), 491-500, doi:10.4319/lo.1992.37.3.0491.

Gordon, H.R., O.B. Brown, R.H. Evans, J.W. Brown, R.C. Smith, K.S. Baker, and D.K. Clark, 1988. A semianalytic radiance model of ocean color. J. Geophys. Res. 93, 10909–10924.

HOBI Labs (Hydro-optics, Biology & Instrumentation Laboratories, Inc.), 2008. HydroScat-4 spectral backscattering sensor, User's manual, Rev. 4, June 15, 2008, 65 pp.

IOCCG, 2006. Remote Sensing of Inherent Optical Properties: Fundamentals, Tests of Algorithms, and Applications, in Reports of the International Ocean-Colour Coordinating Group, No. 5, edited by Z.-P. Lee, p. 126, IOCCG, Dartmouth, Canada.

Lee, Z.P., K.L. Carder, C.D. Mobley, R.G. Steward, and J.S. Patch, 1999. Hyperspectral remote sensing for shallow waters: 2. Deriving bottom depths and water properties by optimization. Appl. Opt. 38, 3831–3843.

Lee, Z.P., K.L. Carder, and R.A. Arnone, 2002. Deriving inherent optical properties from water color: a multiband quasi-analytical algorithm for optically deep waters. Appl. Opt. 41, 5755–5772.

Maffione, R.A., and D.R. Dana, 1997. Instruments and methods for measuring the backward-scattering coefficient of ocean waters. Appl. Opt., 36(24), 6057-6067.

Meler, J., S.B. Woźniak, J. Stoń-Egiert, and B. Woźniak, 2018. Parameterization of phytoplankton spectral absorption coefficients in the Baltic Sea: general, monthly and two-component variants of approximation formulas (Ocean Optics XXIV, electronic version of extended abstract).

Morel, A., 1974. Optical properties of pure water and pure sea water. In: Jerlov, N.G., Nielsen, E.S. (Eds.), Optical Aspects of Oceanography, Academic Press, New York, pp. 1–24.

Pegau, W.S., D. Gray, and J.R.V. Zaneveld, 1997. Absorption and attenuation of visible and near-infrared light in water: Dependence on temperature and salinity. Appl. Opt., 36, 6035– 6046.

Pope, R. M., and E.S. Fry, 1997, Absorption spectrum (380-700 nm) of pure water. II. Integrating cavity measurements, Appl. Opt., 36, 8710-8723.

Smith, R.C., and K.S. Baker, 1981. Optical properties of the clearest natural waters (200–800 nm), Appl. Optics, 20 (2), 177–184, http://dx.doi.org/10.1364/AO.20.000177.

Sogandares, F. M., and E.S. Fry, 1997, Absorption spectrum (340-640 nm) of pure water. I. Photothermal measurements, Appl. Opt., 36, 8699-8709.

Werdell, P.J., L.I.W. McKinna, E. Boss, S.G. Ackleson, S.E. Craig, W.W. Gregg, Z. Lee, S. Maritorena, C.S. Roesler, C.S. Rousseaux, D. Stramski, J.M. Sullivan, M.S. Twardowski, M. Tzortziou, and X. Zhang, 2018. An overview of approaches and challenges for retrieving marine inherent optical properties from ocean color remote sensing, Progress in Oceanography,160, 186-212, https://doi.org/10.1016/j.pocean.2018.01.001.

Zaneveld, J. R. V., J. C. Kitchen, and C. Moore, 1994. The scattering error correction of reflecting-tube absorption meters. Proc. SPIE Int. Soc. Opt. Eng., 2258, 44-55.

Zibordi, G., and G. M. Ferrari, 1995. Instrument self-shading in underwater optical measurements: experimental data. Appl. Opt. 34 (2), 2750—2754, http://dx.doi.org/10.1364/AO.34.002750.

Acknowledgements

Financial support for this research was provided by Statutory Research Programme at the Institute of Oceanology, Polish Academy of Sciences (themes No. I.1 and II.5). Partial support was also provided by the "SatBałtyk" project funded by the European Union through the European Regional Development Fund (contract No. POIG.01.01.02-22-011/09, project entitled "The Satellite Monitoring of the Baltic Sea Environment"), and by the project awarded to S.B.W. by National Science Centre, Poland, entitled "Advanced research into the relationships between optical, biogeochemical and physical properties of suspended particulate matter in the southern Baltic Sea" (contract No. 2016/21/B/ST10/02381). The authors would like to thank their colleagues from IOPAN for help during cruises at sea.

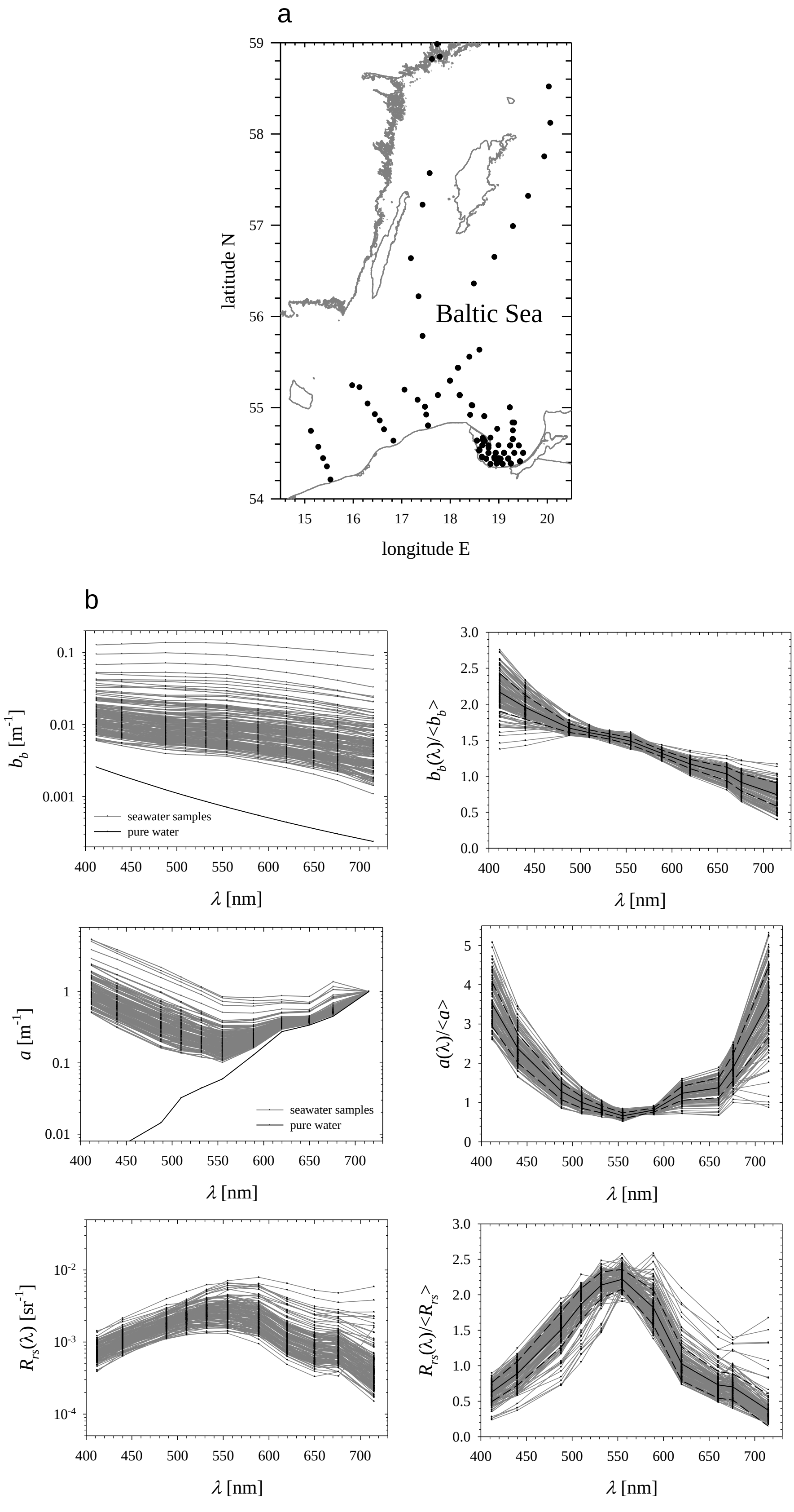

Figure 1. a) Location of sampling stations; b) spectra and normalized spectra of the light backscattering coefficient $b_b(\lambda)$, light absorption coefficient $a(\lambda)$ and remote-sensing reflectance $R_{rs}(\lambda)$ analysed in this work.

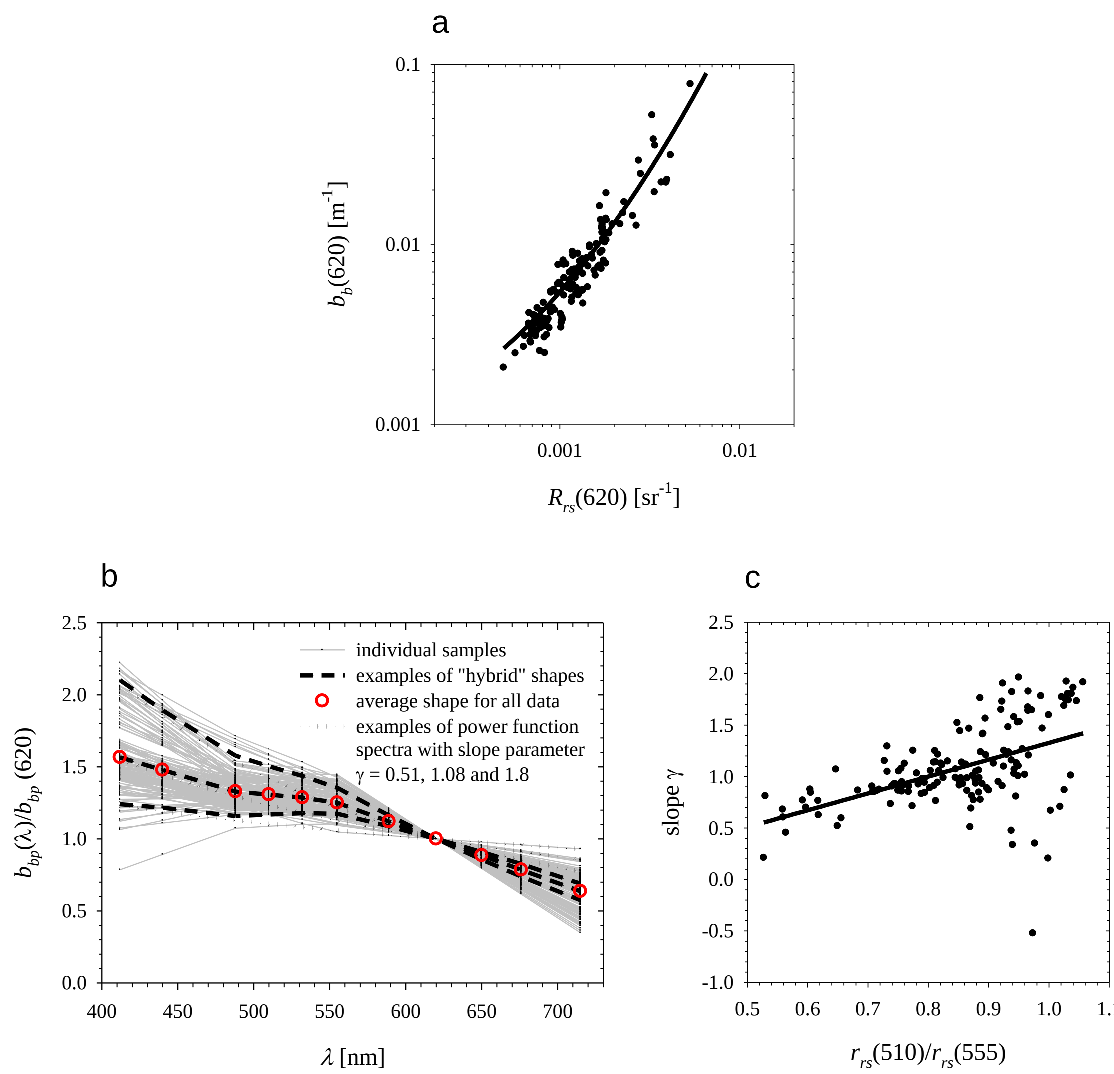

Figure 2. a) The relationship between backscattering coefficient $b_b(620)$ and remote-sensing reflectance $R_{rs}(620)$ and its polynomial approximation (see eq. (1)); b) backscattering coefficient spectra normalized at 620 nm and examples of different approximated spectral shapes (see eq. (2)); c) the relationship between slope parameter γ and reflectance ratio of $r_{sr}(510)/r_{rs}(555)$ and its linear approximation (see eq. (3)).

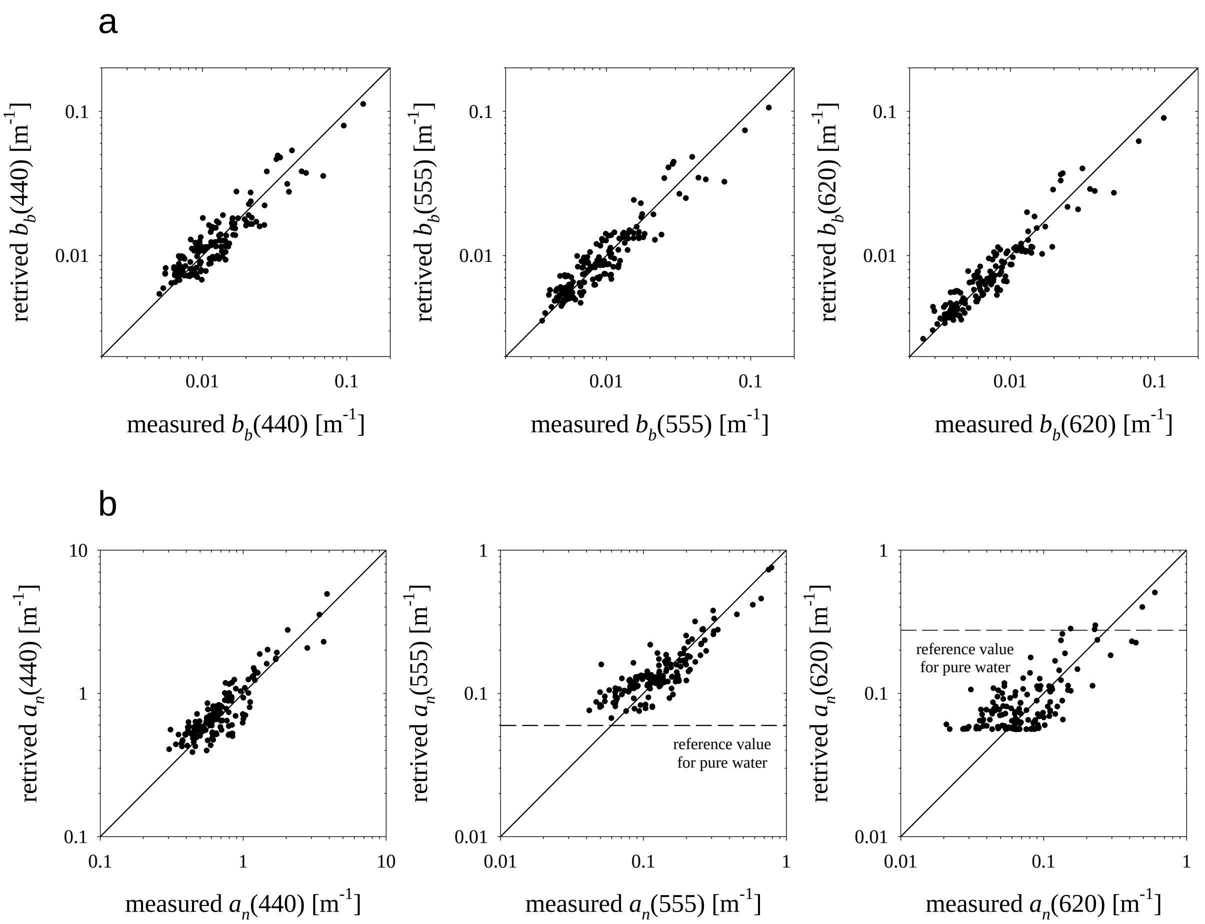

Figure 3. Comparison of retrieved and measured values of optical coefficients for three light wavelengths: a) for the backscattering coefficients $b_b(\lambda)$; b) for the absorption coefficient by non-water constituents of seawater $a_n(\lambda)$.

Table 1. Two examples of simple algorithms for retrieving inherent optical properties of seawater from remote-sensing reflectance spectra. In algorithm A the backscattering coefficient $b_b(620)$ is retrieved directly from reflectance $R_{rs}(620)$, while in algorithm B it is retrieved indirectly through the ratio $u(620)$. Both algorithms in their final steps allow to estimate the absorption coefficient spectra ($a(\lambda)$ and $a_n(\lambda)$) based on retrieved spectra of $b_b(\lambda)$ and $u(\lambda)$.

ALGORITHM A (4 steps)

STEP A1: estimating b_b at the red light wavelength as a function of R_{rs}

$b_b(620) = 10^{(0.4369\ (\log(Rrs(620)))^{\wedge}2\ +\ 3.7597\ (\log(Rrs(620)))\ +\ 5.0813)}$

STEP A2: estimating b_b spectral values

$b_b(\lambda) = (b_b(620) - b_{bw}(620))\ C_1(\lambda)\ (620/\lambda)^{\gamma} + b_{bw}(\lambda)$

where values of C_1 are as follows:

λ	412	440	488	510	532	555	589	620	650	676	715
$C_1(\lambda)$	1.01	1.02	1.02	1.06	1.09	1.11	1.06	1	0.93	0.86	0.74

$\gamma = 1.6379\ (r_{rs}(510)/r_{rs}(555)) - 0.3104$

where $r_{rs}(\lambda) = R_{rs}(\lambda)/(0.52 + 1.7\ R_{rs}(\lambda))$ (simplified formula acc. to Lee et al. (2002))

STEP A3: variants for estimating $u(\lambda)$ as a function of $R_{rs}(\lambda)$ (see also Figure 6a and b))

1st variant: $u(\lambda) = (R_{rs}(\lambda)/0.034)^{(1/0.8275)}$

2nd variant: $u(\lambda) = (-g_0 - [(g_0)^2 + 4g_1\ R_{rs}(\lambda)]^{0.5})/2g_1$, where $g_0 = 0.0686$, $g_1 = -0.1384$

3rd variant: $u(\lambda) = R_{rs}(\lambda)/C_2(\lambda)$

where values of C_2 are as follows:

λ	412	440	488	510	532	555	589	620	650	676	715
$C_2(\lambda)$	0.0607	0.0647	0.0701	0.0715	0.0702	0.0616	0.0681	0.0634	0.0563	0.0848	0.0970

STEP A4: analytically calculating $a(\lambda)$ and $a_n(\lambda)$

$a(\lambda) = b_b(\lambda)[(1/u(\lambda))-1]$

$a_n(\lambda) = a(\lambda) - a_w(\lambda)$

ALGORITHM B (5 steps)

STEP B1: estimating $r_{rs}(\lambda)$ from $R_{rs}(\lambda)$

$r_{rs}(\lambda) = R_{rs}(\lambda)/(0.52 + 1.7\ R_{rs}(\lambda))$ (simplified formula acc. to Lee et al. (2002))

STEP B2: variants for estimating $u(\lambda)$ as a function of $r_{rs}(\lambda)$ (see also Figure 6c)

1st variant: $u(\lambda) = (r_{rs}(\lambda)/0.0641)^{(1/0.8238)}$

2nd variant: $u(\lambda) = (-g_0 - [(g_0)^2 + 4g_1\ r_{rs}(\lambda)]^{0.5})/2g_1$, where $g_0 = 0.1316$, $g_1 = -0.2832$

3rd variant: $u(\lambda) = r_{rs}(\lambda)/C_3(\lambda)$

where values of C_3 are as follows:

λ	412	440	488	510	532	555	589	620	650	676	715
$C_3(\lambda)$	0.116	0.124	0.134	0.136	0.134	0.117	0.130	0.121	0.108	0.163	0.186

STEP B3: estimating b_b at the red light wavelength as a function of u (see also Figure 6d)

$b_b(620) = 10^{(0.5606\ (\log(u(620)))^{\wedge}2\ +\ 3.0844\ (\log(u(620)))\ +\ 1.462)}$

STEP B4: estimating b_b spectral values

(same as STEP A2 of ALG. A)

STEP B5: analytically calculating $a(\lambda)$ and $a_n(\lambda)$

(same as STEP A4 of ALG. A)

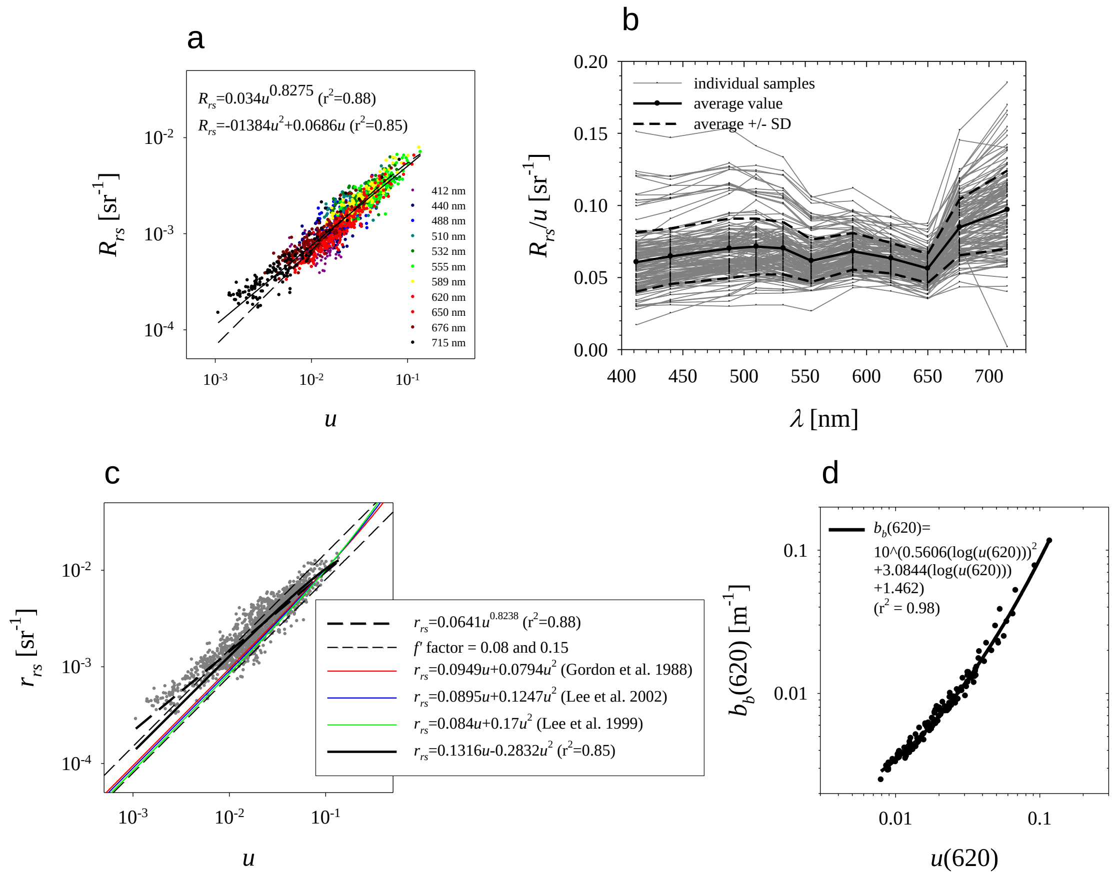

Figure 4. Illustration of the various statistical relationships used in simple algorithms presented here: a) relationship between R_{rs} (above surface reflectance) and u (all data regardless of light wavelength combined together) (approximation equations are given in the panel); b) relationship between the ratio of R_{rs}/u and the light wavelength λ; c) relationship between r_{rs} (below surface reflectance) and u (all data regardless of light wavelength combined together) (approximation equations and literature formulas acc. to Gordon et al, 1988, Lee et al. 1999 and 2002 are given in the panel); d) relationship between $b_b(620)$ and $u(620)$ (approximation equation is given in the panel).

Table 2. Statistical parameters[1] characterizing the quality of $b_b(\lambda)$, $a(\lambda)$ and $a_n(\lambda)$ estimates using different formulas and algorithms: a) for $b_b(\lambda)$ estimated using simple calculation method presented in form of eq. (1) to (3), and for $a(\lambda)$ and $a_n(\lambda)$ estimated according to steps A3 and A4 of algorithm A (step A3, 3rd variant); b) same as a) but for estimates obtained using algorithm B (step B2, 3rd variant); c) same as a) but for estimates obtained using the Quasi-Analytical Algorithm (QAA) (see *e.g.* Lee et al. (2002), IOCCG (2006); for a description of QAA_v6, see: *http://ioccg.org/resources/software/*).

a) algorithm A

Retrieved quantity	wavelength [nm]	412	440	488	510	532	555	589	620	650	676	715
$b_b(\lambda)$	*sys.err.*[%]	0.5	0.2	-0.1	-0.1	0.0	0.0	-0.1	-0.1	-0.1	0.2	1.5
	X	**1.26**	1.26	1.25	1.25	1.26	1.26	1.25	1.24	**1.23**	1.23	**1.28**
$a(\lambda)$	*sys.err.*[%]	5.8	4.5	4.0	3.5	3.4	2.9	1.7	1.3	1.6	2.9	
	X	**1.28**	1.24	1.26	1.27	1.21	1.21	1.18	1.11	**1.09**	1.20	
$a_n(\lambda)$	*sys.err.*[%]	5.8	4.6	4.2	4.4	4.6	6.5	8.7	11.8			
	X	1.28	**1.25**	1.27	1.31	1.27	**1.34**	1.46	1.51			

b) algorithm B

Retrieved quantity	wavelength [nm]	412	440	488	510	532	555	589	620	650	676	715
$b_b(\lambda)$	*sys.err.*[%]	-1.6	-1.9	-2.3	-2.3	-2.3	-2.3	-2.4	-2.5	-2.4	-2.2	-0.9
	X	**1.26**	1.26	1.25	1.25	1.26	1.26	1.25	1.24	**1.23**	1.24	**1.29**
$a(\lambda)$	*sys.err.*[%]	3.6	2.2	1.6	1.2	1.0	0.5					
	X	**1.27**	1.24	1.25	1.27	1.20	1.21					
$a_n(\lambda)$	*sys.err.*[%]	3.6	2.3	1.8	1.7	1.7	3.0					
	X	1.27	**1.24**	1.27	1.31	1.26	**1.34**					

c) algorithm QAA_v6

Retrieved quantity	wavelength [nm]	412	440	488	510	532	555	589	620	650	676	715
$b_b(\lambda)$	*sys.err.*[%]	-2.1	0.4	6.4	6.6	6.9	8.4	17.8	28.9	42.8	58.7	93.6
	X	**1.27**	1.27	1.27	1.27	1.27	1.27	1.26	**1.25**	1.25	1.25	1.29
$a(\lambda)$	*sys.err.*[%]	-13.5	-21.0	-22.0	-21.5		-7.2					
	X	**1.33**	1.31	1.33	1.34		**1.28**					
$a_n(\lambda)$	*sys.err.*[%]	-13.6	-21.2	-22.9	-24.3		-9.1					
	X	1.34	**1.31**	1.35	1.41		**1.46**					

[1]The following logarithmic statistics parameters are presented here:

the systematic error: $sys.err. = 10^{\langle \log\left(\frac{P_i}{O_i}\right)\rangle} - 1$; $\langle \log\left(\frac{P_i}{O_i}\right)\rangle = \frac{1}{n}\sum_{i=1}^{n} \log\left(\frac{P_i}{O_i}\right)$,

where P_i, O_i - predicted and observed values, respectively;

the standard error factor: $X = 10^{\sigma_{log}}$; $\sigma_{log} = \left[\frac{1}{n-1}\sum_{i=1}^{n}\left(\log\left(\frac{P_i}{O_i}\right) - \frac{1}{n}\sum_{j=1}^{n}\log\left(\frac{P_j}{O_j}\right)\right)^2\right]^{\frac{1}{2}}$;

X allows to quantify the range of the statistical error, which extends from the value of σ–=(1/*X*)-1 to the value of σ+=*X*-1.